# Defective Skeletogenesis with Kidney Stone Formation in Dwarf Zebrafish Mutant for *trpm7*

Michael R. Elizondo,[1,4] Brigitte L. Arduini,[2]
Jennifer Paulsen,[3] Erin L. MacDonald,[1]
Jaime L. Sabel,[3] Paul D. Henion,[2,*]
Robert A. Cornell,[3,*] and David M. Parichy[1,4,*]
[1]Section of Integrative Biology and
Section of Molecular, Cell and Developmental Biology
Institute for Cellular and Molecular Biology
University of Texas at Austin
1 University Station C0930
Austin, Texas 78712
[2]Center for Molecular Neurobiology and
Department of Neuroscience
Ohio State University
105 Rightmire Hall, 1060 Carmack Rd.
Columbus, Ohio 43210
[3]Department of Anatomy and Cell Biology
Roy and Lucille Carver College of Medicine
1-532 Bowen Science Building
University of Iowa
Iowa City, Iowa 52242

## Summary

Development of the adult form requires coordinated growth and patterning of multiple traits in response to local gene activity as well as to global endocrine and physiological effectors. An excellent example of such coordination is the skeleton. Skeletal development depends on the differentiation and morphogenesis of multiple cell types to generate elements with distinct forms and functions throughout the body [1–3]. We show that zebrafish *touchtone/nutria* mutants exhibit severe growth retardation and gross alterations in skeletal development in addition to embryonic melanophore and touch-response defects [4, 5]. These alterations include accelerated endochondral ossification but delayed intramembranous ossification, as well as skeletal deformities. We show that the *touchtone/nutria* phenotype results from mutations in *trpm7*, which encodes a transient receptor potential (TRP) family member that functions as both a cation channel and kinase. We find *trpm7* expression in the mesonephric kidney and show that mutants develop kidney stones, indicating renal dysfunction. These results identify a requirement for *trpm7* in growth and skeletogenesis and highlight the potential of forward genetic approaches to uncover physiological mechanisms contributing to the development of adult form.

## Results and Discussion

Genetic screens for ethyl-*N*-nitrosourea-induced mutations affecting zebrafish postembryonic development

*Correspondence: henion.1@osu.edu (P.H.); robert-cornell@uiowa.edu (R.C.); dparichy@u.washington.edu (D.P.)
[4]Present address: Department of Biology, University of Washington, Box 351800, Seattle, Washington 98195.

uncovered the *nutria^{j124e2}* mutant, named for its small size, odd shape, and tendency to swim near the surface (Figures 1A and 1B). As embryos and early larvae (2–5 days post fertilization [dpf]), *nutria* are comparable in size to wild-type siblings, but during later development they exhibit a severe growth deficit (Figure 1C). Craniofacial and trunk body proportions are altered, although other external features (e.g., scales, fins, and the complement of adult pigment cells) are not grossly abnormal. To identify the locus causing this dwarf phenotype, we mapped the *nutria* mutation to chromosome 18 in the vicinity of *touchtone* (*tct*) [4, 5]. Both *tct* and *nutria* mutants exhibit embryonic melanophore deficiencies and touch unresponsiveness prior to hatching. Complementation tests confirmed that *nutria* and *tct* are allelic. Fine mapping of the critical region revealed, among other genes, *trpm7*, which encodes an ortholog of the transient receptor potential (TRP) melastatin-7 dual-function cation channel and kinase (0/2889 recombinants) [6]. Although *TRPM7* has not been implicated in growth previously, a member of this family, *TRPM1* (*melastatin*), is expressed in human melanocytic nevi [7], and zebrafish melanophores require *tct* cell autonomously [4, 5].

Our data show that *trpm7* corresponds to *tct*. Sequencing *trpm7* cDNAs revealed premature stop codons in the severe alleles *tct^{j124e1}* and *tct^{b508}* (see the Supplemental Data available with this article online). Moreover, the injection of wild-type embryos with a *trpm7* splice-blocking morpholino oligonucleotide results in both melanophore deficiencies and touch unresponsiveness and thus phenocopies the mutant (see Supplemental Data). Finally, TRPM7 acts as an inwardly rectifying cation channel with broad specificity but high affinity for $Mg^{2+}$ and $Ca^{2+}$, suggesting that manipulating divalent-cation availability might rescue embryonic phenotypes of *trpm7* mutants [8, 9]. Supplemental $Mg^{2+}$ partially rescued melanophore development, whereas supplemental $Ca^{2+}$ partially rescued melanophore development and touch responsiveness (Figures 1D–1F; Supplemental Data). Thus, *trpm7* is the gene affected in *tct* mutants.

To clarify the mode(s) of *trpm7* activity, we examined *trpm7* expression in wild-type embryos and larvae. Consistent with previous observations, we detected widespread *trpm7* expression at embryonic stages, including in the central nervous system, pronephros, lens, and other tissues [10] (data not shown). In metamorphic larvae, transcripts were abundant in liver, mesonephric kidney tubules, and corpuscles of Stannius, which are teleost glands that contribute to calcium homeostasis [11] (Figures 2A–2C). In contrast to severe alleles, *trpm7^{j124e2}* (*nutria*) individuals are viable, allowing us to assess functional consequences of *trpm7* mutation during postembryonic development. Consistent with kidney expression of *trpm7*, histological examination of *trpm7^{j124e2}* mutant larvae revealed mineralization within mesonephric tubules (Figures 2D and 2F). These data suggest that altered *trpm7* function in the kidney, in corpuscles of Stannius, or in both af-
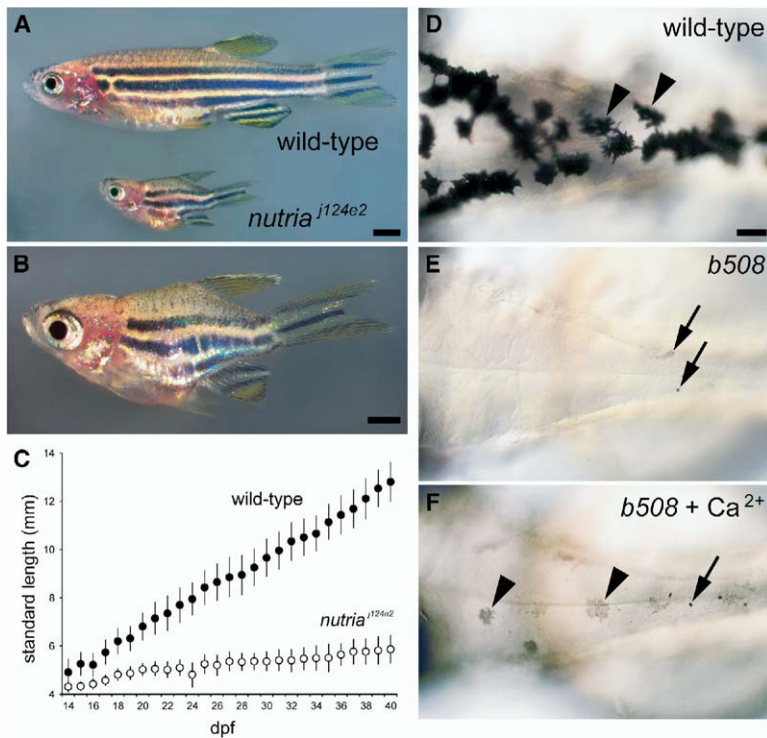
Figure 1. Retarded Growth and Altered Body Proportions in *nutria* (*tct*) Mutant Zebrafish with Embryonic Melanophore Defect Rescuable by Divalent-Cation Supplementation

(A) Wild-type and *nutria* siblings, 50 dpf.

(B) Higher-magnification image of a *nutria* mutant.

(C) Diminished growth of *nutria* compared to wild-type siblings. Each point shows the mean standard length ± standard deviation for seven to 20 individuals.

(D–F) Embryonic melanophore defects are rescuable with supplemental $Ca^{2+}$. (D) Wild-type embryos exhibit well-melanized and well-spread melanophores (arrowheads). (E) Mutants exhibit few poorly melanized and punctate melanophores or melanophore fragments (arrows); *tct*[b508] is shown. (F) In a medium supplemented with $Ca^{2+}$, mutant melanophores are more numerous, spread, and melanized (arrowheads), although some punctate melanophores remain (arrow).

Scale bars represent the following: (A), 2 mm; (B), 1 mm; (D–F), 100 $\mu$m.

fects whole-organism cation homeostasis and leads to nephrolithiasis.

Because dwarfism syndromes in humans are associated with a range of skeletal defects [12] and cation homeostasis affects bone development and maintenance [13], we asked whether the growth deficit and disproportionality of *trpm7*[j124e2] mutants is associated with changes in ossification. A comprehensive analysis of 87 bones between 9 and 51 dpf revealed extensive alterations in ossification sequence between wild-type and mutant larvae (Figures 3 and 4). Among numerous examples of sequence reordering is the epural bone of the caudal fin, which is the 78th bone to ossify in wild-type larvae but only the 32nd to ossify in *trpm7* mutant larvae. Conversely, the maxilla is the 15th bone to ossify in wild-type larvae but the 40th to ossify in *trpm7* mutant larvae. Thus, *trpm7*+ is essential for the normal sequence of ossification.

To better understand ossification changes, we categorized bones according to function and anatomical location as well as cellular origin. The most dramatic differences were between endochondral bones, which develop through mineralization of a cartilage model, and intramembranous bones, which develop directly, without a cartilage model [1, 14, 15]. In *trpm7* mutants, endochondral bones (red connectors in Figure 4A) appeared on average earlier in the ossification sequence than they did in wild-type larvae, whereas intramembranous bones (green connectors) appeared on average later than they did in wild-type larvae. Dissociation of endochondral and intramembranous ossification is exemplified by the caudal complex, in which the endochondral hypurals and epural ossify much earlier in *trpm7* mutants compared to the wild-type, whereas the

intramembranous urostyle, centra, and other bones ossify much later in *trpm7* mutants compared to the wild-type (Figures 3A–3H). Precocious endochondral ossification is similarly evident in the suspensorium and the branchial arches of *trpm7* mutants (Figures 3I–3P), whereas delayed intramembranous ossification is apparent for several bones of the anterior head (Figures 3Q–3V). The accelerated ossification of endochondral bones and the delayed ossification of intramembranous bones reflect order in the ossification sequence as well as absolute timing. One can most easily visualize these timing differences by plotting how genotype affects the likelihood of bones being ossified at any given age against the statistical significance of these differences (Figures 4B and 4C). Defects in ossification timing do not simply reflect growth retardation; even severely runted wild-type fish develop skeletal elements of normal shape without premature ossification (Supplemental Data).

Furthermore, functional-anatomical units in close proximity were found to be differentially affected, even after we controlled for the relative contributions of endochondral and intramembranous bones within these units. For example, otic bones are accelerated, whereas orbital bones are delayed, despite the anatomical proximity of these bones and their similar endochondral and intramembranous compositions (Figure 4C; Table S1). Finally, *trpm7* mutants exhibited skeletal dysplasia, including extreme malformation of the Weberian (auditory) apparatus and the ribs, compressed vertebrae (of normal number), and kinks in the posterior vertebral column (Figures 3D, 3H, 3S, and 3W).

We have demonstrated that *trpm7* is essential for growth and skeletogenesis during the zebrafish larval-
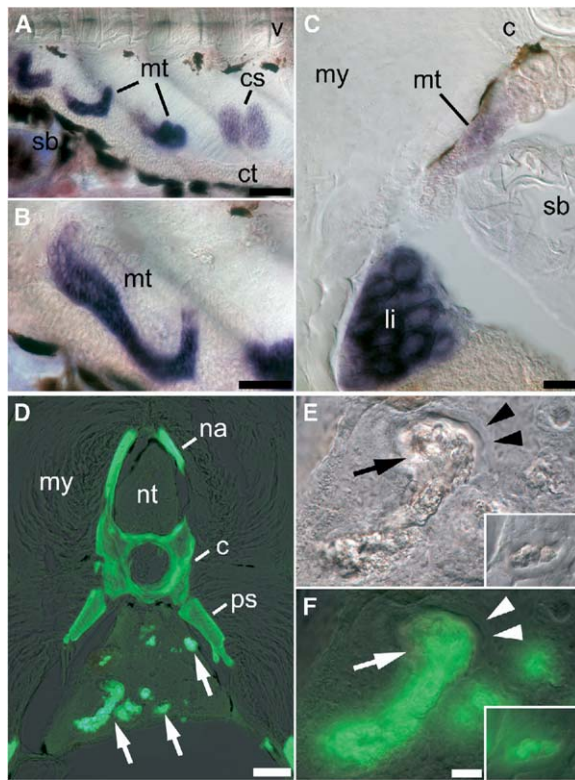
Figure 2. *trpm7* Expression in Wild-Type Larvae and Kidney Stone Formation in *trpm7* Mutants

(A–C) *trpm7* expression in metamorphosing wild-type larvae. (A) At early stages of metamorphosis (14 dpf), *trpm7* mRNA is present in mesonephric tubules (mt) and corpuscles of Stannius (cs). The following abbreviations are used: v, vertebral column; sb, swimbladder; and ct, mesonephric collecting tubule. *trpm7* expression is also detectable in more-anterior regions of the mesonephros (not shown). (B) A higher-magnification *trpm7*⁺ mesonephric tubule is shown. (C) Transverse section of late-metamorphic (24 dpf) larva. *trpm7* transcripts are present in mesonephric tubules and liver (indicated by "li"). *trpm7* transcripts are not detectable in developing endochondral or intramembranous bones. "my" denotes myotome and "c" denotes centrum.

(D–F) *trpm7*$^{j124e2}$ (*nutria*) mutants develop kidney stones. (D) Calcein staining reveals skeletal elements (na, c, ps) and ectopic mineralization (arrows). The following abbreviations are used: na, neural arches; c, centrum; ps, pleural spines; and nt, neural tube. (E) shows left-most ectopic mineralization from panel (D). Epithelium (arrowheads) surrounds the mineralized deposit (arrow). The inset shows mineralized deposit within collecting tubule of another larva. (F) shows calcein staining of mineralized deposits shown in panel (E) and the inset.

Scale bars represent the following: (A), 60 µm; (B), 40 µm; (C) and (D), 80 µm; (E) and (F), 20 µm (15 µm for insets).

to-adult transition and for melanophore development and touch response during embryogenesis. *trpm7* expression in kidney and corpuscles of Stannius, as well as the presence of kidney stones in *trpm7* mutants, support a model in which effects on growth and skeletogenesis reflect physiological regulation of cation homeostasis. These effects may be analogous to those of parathyroid hormone/parathyroid hormone receptor type 1 (PTHR1) regulation of calcium homeostasis in mammals, in which changes in PTHR1 signaling or

downstream effectors such as Runx2 can lead to premature endochondral ossification [16–19]. However, this model does not readily explain the delayed intramembranous ossification observed in *trpm7* mutants. Although the precise functions of *trpm7* in promoting normal ossification sequence and timing, as well as melanophore development and touch response, remain to be elucidated, our analyses reveal important roles for *trpm7* in the physiological regulation of postembryonic growth and skeletogenesis.

**References**

1. Karsenty, G., and Wagner, E.F. (2002). Reaching a genetic and molecular understanding of skeletal development. Dev. Cell *2*, 389–406.
2. Fisher, S., Jagadeeswaran, P., and Halpern, M.E. (2003). Radiographic analysis of zebrafish skeletal defects. Dev. Biol. *264*, 64–76.
3. Kronenberg, H.M. (2003). Developmental regulation of the growth plate. Nature *423*, 332–336.
4. Cornell, R.A., Yemm, E., Bonde, G., Li, W., d'Alencon, C., Wegman, L., Eisen, J., and Zahs, A. (2004). Touchtone promotes survival of embryonic melanophores in zebrafish. Mech. Dev. *121*, 1365–1376.
5. Arduini, B.L., and Henion, P.D. (2004). Melanophore sublineage-specific requirement for zebrafish touchtone during neural crest development. Mech. Dev. *121*, 1353–1364.
6. Wolf, F.I. (2004). TRPM7: Channeling the future of cellular magnesium homeostasis? Sci. STKE *2004*, pe23.
7. Duncan, L.M., Deeds, J., Hunter, J., Shao, J., Holmgren, L.M., Woolf, E.A., Tepper, R.I., and Shyjan, A.W. (1998). Down-regulation of the novel gene melastatin correlates with potential for melanoma metastasis. Cancer Res. *58*, 1515–1520.
8. Monteilh-Zoller, M.K., Hermosura, M.C., Nadler, M.J., Scharenberg, A.M., Penner, R., and Fleig, A. (2003). TRPM7 provides an ion channel mechanism for cellular entry of trace metal ions. J. Gen. Physiol. *121*, 49–60.
9. Schmitz, C., Perraud, A.L., Johnson, C.O., Inabe, K., Smith, M.K., Penner, R., Kurosaki, T., Fleig, A., and Scharenberg, A.M. (2003). Regulation of vertebrate cellular Mg²⁺ homeostasis by TRPM7. Cell *114*, 191–200.
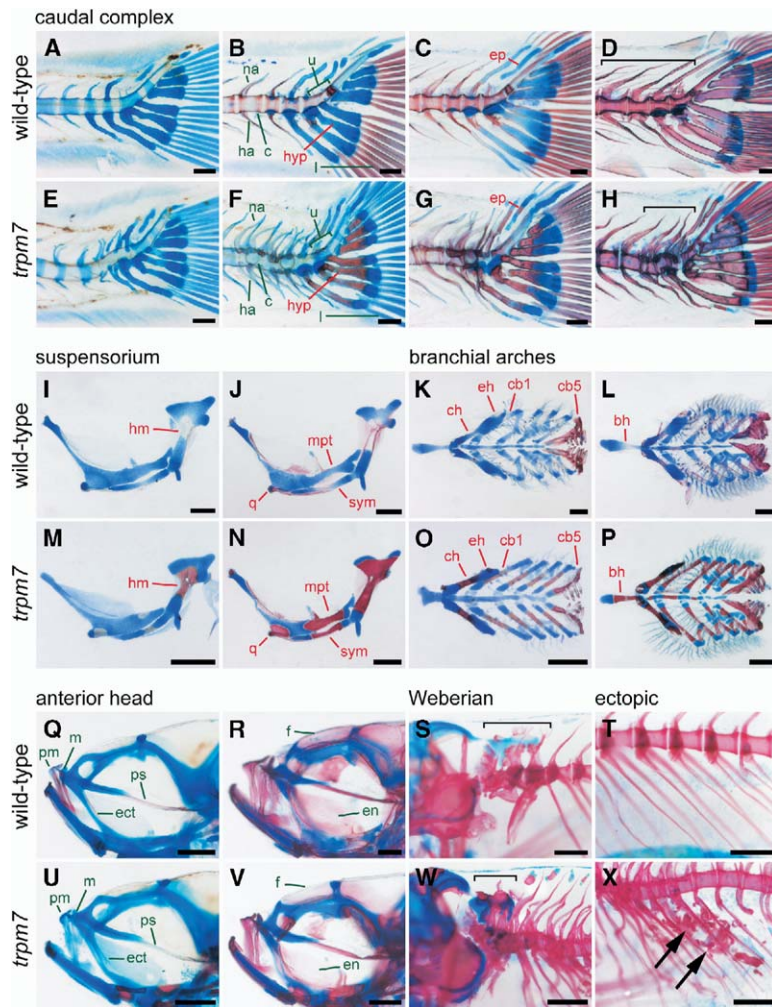
**Figure 3. trpm7^{j124e2} Mutants Exhibit Dramatic Differences in Skeletal Development in Comparison to Wild-Type**

Alizarin red stains ossified bone and mineralized tissues. Alcian blue stains cartilage. Endochondral bone labels are red, and intramembranous bone labels are green.

(A–H) Differences in ossification timing in the caudal complex between wild-type (A–D) and mutant (E–H) siblings (9–44 dpf, left to right). In mutants, endochodondral bones ossify earlier [panels (B) and (F): hyp. Panels (C) and (G): ep], whereas intramembranous bones ossify later [panels (B) and (F): na, u, ha, c, l]. Compression of vertebrae and the caudal complex are evident [panels (D) and (H): brackets].

(I–P) The suspensorium (I–N) and branchial arches (K–P) illustrate precocious endocondral ossification in mutants. Advances in ossification are apparent for several endochondral bones at early stages [17 dpf. Panels (I) and (M): hm. Panels (K) and (O): ch, eh, cb1] and later stages [47 dpf. Panels (J) and (N): mpt, q, sym. Panels (L) and (P): bh].

(Q, U, R, V) Bones of the anterior head illustrate delayed intramembranous ossification in mutants. Intramembranous bones are delayed in mutants at early stages [24 dpf. Panels (Q) and (U): pm, m, ps, ect] and later stages [44 dpf. Panels (R) and (V): f, en].

(S, W) Bones of the Weberian apparatus (brackets) are malformed and compressed in mutants.

(T, X) Mineralizations within the mesonephros of mutant larvae [arrowheads in panel (X)].

(S) and (T) are at 35 dpf; (W) and (X) are at 30 dpf. The following abbreviations are used: bh, basihyal; c, centra; cb1, ceratobranchial 1; cb5, ceratobranchial 5; ch, ceratohyal; ect, ectopterygoid; eh, epihyal; en, entopterygoid; ep, epural; f, frontal; ha, hemal arches; hm, hyomandibula; hyp, hypurals; l, lepidotrichia; m, maxilla; mpt, metapterygoid; na, neural arches; pm, premaxilla; ps, parasphenoid; q, quadrate; sym, symplectic; and u, urostyle and ural 1 + 2.

Scale bars represent the following: (A–H), 100 μm; (I–X), 250 μm.

10. The Zebrafish Information Network. 2005. (http://zfin.org).
11. Krishnamurthy, V.G. (1976). Cytophysiology of corpuscles of Stannius. Int. Rev. Cytol. 46, 177–249.
12. Hall, C.M. (2002). International nosology and classification of constitutional disorders of bone (2001). Am. J. Med. Genet. 113, 65–77.
13. Dvorak, M.M., and Riccardi, D. (2004). Ca²⁺ as an extracellular signal in bone. Cell Calcium 35, 249–255.
14. Cubbage, C.C., and Mabee, P.M. (1996). Development of the cranium and paired fins in the zebrafish Danio rerio (ostariophysi, Cyprinidae). J. Morphol. 229, 121–160.
15. Bird, N.C., and Mabee, P.M. (2003). Developmental morphology of the axial skeleton of the zebrafish, Danio rerio (Ostariophysi: Cyprinidae). Dev. Dyn. 228, 337–357.
16. Schipani, E., Kruse, K., and Juppner, H. (1995). A constitutively active mutant PTH-PTHrP receptor in Jansen-type metaphyseal chondrodysplasia. Science 268, 98–100.
17. Karaplis, A.C., He, B., Nguyen, M.T., Young, I.D., Semeraro, D., Ozawa, H., and Amizuka, N. (1998). Inactivating mutation in the human parathyroid hormone receptor type 1 gene in Blomstrand chondrodysplasia. Endocrinology 139, 5255–5258.
18. Takeda, S., Bonnamy, J.P., Owen, M.J., Ducy, P., and Karsenty, G. (2001). Continuous expression of Cbfa1 in nonhypertrophic chondrocytes uncovers its ability to induce hypertrophic chondrocyte differentiation and partially rescues Cbfa1-deficient mice. Genes Dev. 15, 467–481.
19. Ueta, C., Iwamoto, M., Kanatani, N., Yoshida, C., Liu, Y., Enomoto-Iwamoto, M., Ohmori, T., Enomoto, H., Nakata, K., Takada, K., et al. (2001). Skeletal malformations caused by overexpression of Cbfa1 or its dominant negative form in chondrocytes. J. Cell Biol. 153, 87–100.
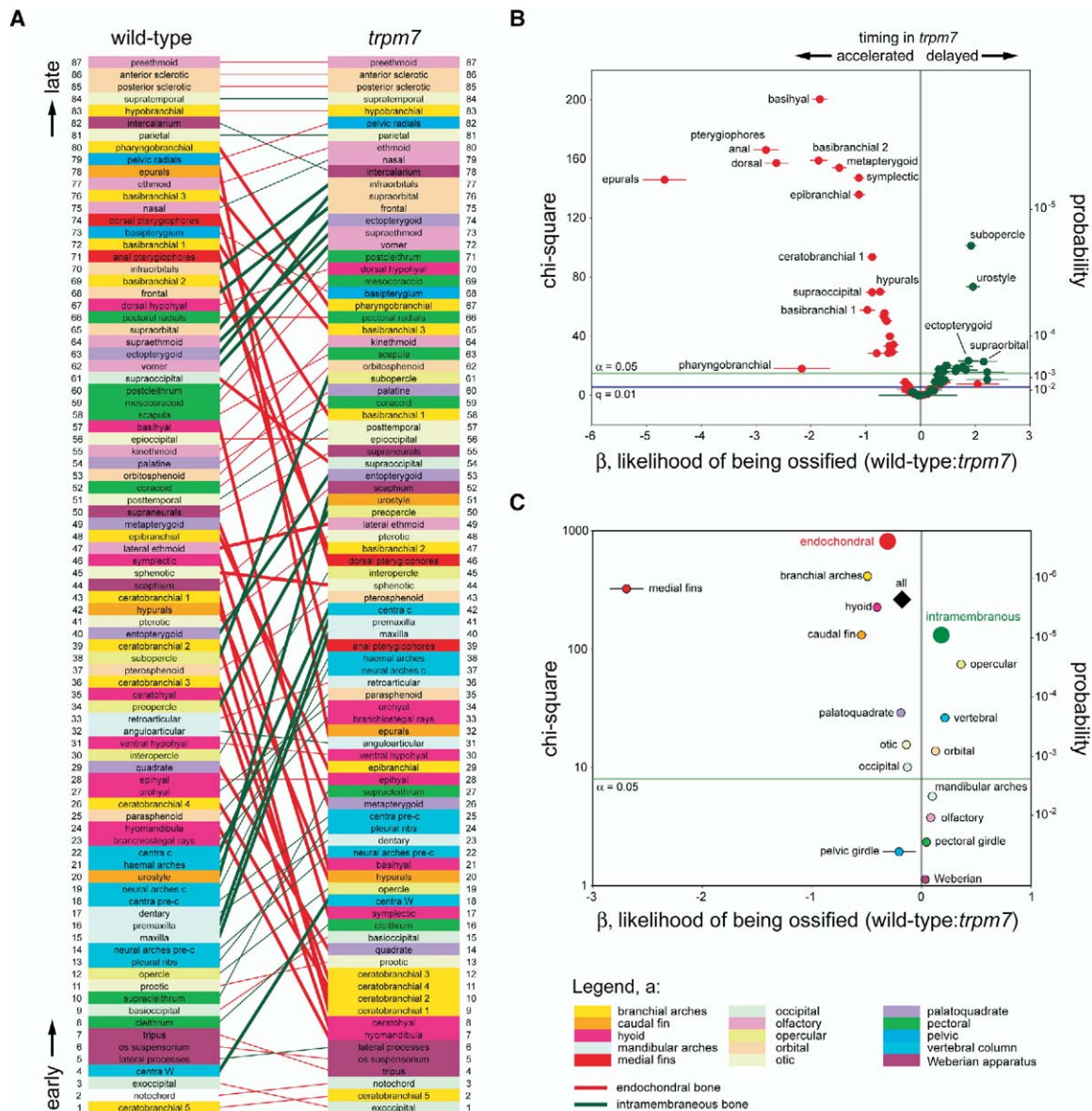
**Figure 4. Altered Sequence and Timing of Skeletal Ossification in *trpm7*[j124e2] Compared to the Wild-Type**

Wild-type larvae (*n* = 500) and *trpm7* mutant siblings (*n* = 431) were scored for ossification of 87 bones, yielding 80,997 ossification scores. Schematics of bone locations, functional-anatomical units, and effects for each bone are in the Supplemental Data.

(A) In mutants, endochondral bones (red connectors) appear on average earlier in the ossification sequence, whereas intramembranous bones (green connectors) appear on average later in the ossification sequence. Bold connectors show bones in which ossification timing, in addition to sequence, was significantly altered [panel (B)].

(B) In mutants, analyses by developmental mode reveal accelerated ossification for many endochondral bones (red) but delayed ossification for many intramembranous bones (green). The *x* axis shows the relative likelihood of ossification in the wild-type compared to the mutant: estimates greater than 0 indicate that the bone is more likely to be ossified in wild-type, and ossification is therefore delayed in the mutant; estimates less than 0 indicate that the bone is less likely to be ossified in wild-type fish, and ossification is therefore accelerated in the mutant. The *y* axis shows statistical significance by chi-square value (left axis) and p value (right axis). $\alpha$ = 0.05 and q = 0.01 are the thresholds of statistical significance after multiple comparisons were controlled for.

(C) Analyses by functional-anatomical unit and developmental mode. Functional-anatomical units were differentially affected in the mutants even after their relative endochrondral and intramembranous compositions were controlled for. Averages: of all bones, diamond; of endocondral bones, large red point; of intramembranous bones, large green point.

Error bars in (B) and (C) show one standard error for logistic regression coefficients, $\beta$.